Photosynth Res
DOI 10.1007/s11120-016-0264-8

ORIGINAL ARTICLE

Structural modeling of the phycobilisome core and its association with the photosystems

D. V. Zlenko[1] · Pavel M. Krasilnikov[1] · Igor N. Stadnichuk[2]

Received: 31 December 2015 / Accepted: 14 April 2016

Abstract The phycobilisome (PBS) is a major light-harvesting complex in cyanobacteria and red algae. To obtain the detailed structure of the hemidiscoidal PBS core composed of allophycocyanin (APC) and minor polypeptide components, we analyzed all nine available 3D structures of APCs from different photosynthetic species and found several variants of crystal packing that potentially correspond to PBS core organization. Combination of face-to-face APC trimer crystal packing with back-to-back APC hexamer packing suggests two variants of the tricylindrical PBS core. To choose one of these structures, a computational model of the PBS core complex and photosystem II (PSII) dimer with minimized distance between the terminal PBS emitters and neighboring antenna chlorophylls was built. In the selected model, the distance between two types of pigments does not exceed 37 Å corresponding to the Förster mechanism of energy transfer. We also propose a model of PBS and photosystem I (PSI) monomer interaction showing a possibility of supercomplex formation and direct energy transfer from the PBS to PSI.

Keywords Allophycocyanin · Phycobilisome core · Photosystems II and I

✉ D. V. Zlenko
dvzlenko@gmail.com

[1] Biological faculty, M.V. Lomonosov Moscow State University, Lenin hills, 1/12, Moscow, Russia 119991

[2] K.A. Timiryazev Institute of Plant Physiology RAS, Botanicheskaya st, 35, Moscow, Russia 127276

Introduction

According to a study of Gantt and Conti (1966), phycobiliproteins (PBPs) are localized in giant macromolecular complexes—phycobilisomes (PBSs)—associated with the cytoplasmic in cyanobacteria and stromal in red algae surface of the thylakoid membranes. There are three main groups of PBPs: allophycocyanin (APC), phycocyanins, and phycoerythrins. They consist of α and β chromophorylated polypeptide subunits in 1:1 ratio self-associating in $(\alpha\beta)$-heteromonomers. In solution, $(\alpha\beta)$-monomers further form threefold symmetric disk-shaped $(\alpha\beta)_3$-trimers and $(\alpha\beta)_6$-hexamers. In vivo, these disks are stacked into cylinders, which in turn form the native PBS particle. This is driven by a number of PBS linker proteins not having chromophores. Besides the structural function, the minor linker polypeptides serve for optimization of the absorbance and energy transfer characteristics of PBS (Bryant et al. 1979; Liu et al. 2005; Stadnichuk et al. 2015). The native PBS can have a molecular weight of more than 5 MDa containing up to one hundred $(\alpha\beta)_3$-trimer units. Native self-assembly of PBS is remarkable in its accuracy and efficiency in the production of an intricate multi-subunit molecular machine. The most carefully studied tricylindrical hemidiscoidal PBSs are present in many cyanobacterial (Gantt et al. 2003) and some red algae (Reuter et al. 1990) species and consist of two architectural domains: a central tricylindrical core and six cylindrical rods of variable length emanating fan-like from the core. The light energy absorbed by chromophores migrates down the lateral rods into the core, then to the antennal chlorophylls, and finally to the reaction centers of photosystems II and I (PSII and PSI) (Glazer 1984; Rakhimberdieva et al. 2001).

Biochemistry, electron microscopy, and molecular genetics have firmly established the molecular architecture

Published online: 27 April 2016

of the cyanobacterial hemidiscoidal PBS core, which is of particular interest (Bryant 1991; Sidler 1994; Adir 2005; Watanabe and Ikeuchi 2013). The core subcomplex consists of two tightly packed basal cylinders associated with the thylakoid membrane surface and one upper cylinder in parallel with them. Each of the core cylinders is formed by four stacked APC trimers. The chromophores of APCs are covalently bound to highly conserved cysteine residues $\alpha 84$ and $\beta 84$. Bearing altogether 78 polypeptides and 72 phycocyanobilin molecules (Sidler 1994; Adir 2005; Watanabe and Ikeuchi 2013), the core structure has molecular mass of about 1.2 MDa, which is very large even if compared with the mass of the complete PBS. The external APC trimers of cylinders are stabilized by a small 7.8 kDa colorless linker protein (L_C) (Glazer 1984; Reuter et al. 1999). The other minor components of the PBS core are three long-wavelength chromophorylated polypeptides, each present in two copies: ApcD (α-subunit of allophycocyanin B), ApcF (β^{18}-polypeptide), and ApcE (L_{CM} or anchor protein). Similarly to both types of APC subunits, all three minor components carry the same phycocyanobilin molecule. Each of the components is incorporated into one of the basal cylinders and participates as terminal emitter in energy transfer from the core to the photosynthetic reaction centers. The fluorescence emission peaks of ApcD, ApcE, and ApcF are considerably red-shifted compared to the bulk population of APC (Glazer 1984; Sidler 1994; Stadnichuk et al. 2015). In one of the outer trimers of each basal cylinder, one αAPC subunit is replaced with an ApcD polypeptide. In the neighboring trimer, one αAPC subunit is substituted with the chromophorylated PB domain of L_{CM} polypeptide, and the adjoined βAPC subunit is replaced with the ApcF polypeptide. Therefore, there are four different kinds of APC trimers in the PBS core: #1: $(\alpha\beta)_3$, #2: $(\alpha\beta)_3$ L_C, #3: $(\alpha\beta)_2$(ApcD/β) L_{CM}, and #4: $(\alpha\beta)_2$(PBL$_{CM}$/ApcF). The upper cylinder composition is 2:1:1:2, while the composition of the basal cylinders is 2:1:4:3. Two basal core cylinders are arranged in antiparallel fashion and the order of trimers in the second cylinder is 3:4:1:2 (Lundell and Glazer 1983; Anderson and Eiserling 1986; Reuter et al. 1990).

The overall morphology of PBS was investigated through negative staining using electron microscopy (Gantt et al. 2003). Imaging of samples showed clear side, top, and triangular face structural layouts of isolated PBS cores as well as of complete hemidiscoidal PBSs. The structure of the entire PBS was studied to resolution of 13 Å using single-particle electron microscopy (Arteni et al. 2009), which revealed the antiparallel fashion of the two basal cylinders found earlier by biochemical methods. However, the diameter of the discoidal trimer blocks is about 11 nm, which makes the resolution of electron microscopy techniques far from sufficient to describe most of the important details of the PBS core substructure that are of particular interest. The fine crystal structure of the PBS core is also not yet obtained and probably will not be obtained in the near future as the smooth structure of the PBS and hydrophobicity of the large L_{CM} polypeptide significantly complicate the crystallization process. It is generally accepted that the multi-domain ApcE polypeptide ties up all the core components and takes part in the association of the PBS with the thylakoid membrane. Recently, two different entire PBSs were crystallized, but the structure of the PBS remained unresolved due to random positioning of the core components in the crystal (David et al. 2014). Nevertheless, it is known that various proteins often pack in the crystal lattice in a fashion reminiscent of their existence in vivo. Many individual trimers and hexamers of different PBPs have been crystallized. In particular, C-phycocyanin was demonstrated to form rod-like structures in the crystal lattice, which may be identical to the rods found in vivo, albeit lacking linker proteins (Adir 2005; David et al. 2011). The structures of many different APCs were also revealed using X-ray technique.

In the current study, we develop a detailed molecular model of the PBS core based on the available APC crystal structures. Our reconstruction of the PBS core is based on the assumption that all its structural blocks except amorphous parts of ApcE can be found in different APC crystals. Combining structure elements from APC crystals obtained from different species of cyanobacteria and one red alga, we reconstruct the overall three-dimensional structure of an intact PBS core. We also determine the global distribution of all the core subunits including ApcD and the PBL$_{CM}$ domain of ApcE. Besides, our results suggest the molecular architecture of pigment–protein supercomplexes of the PBS with PSII and PSI.

Methods

All the considered 3D structures were obtained from Protein Data Bank (http://www.rcsb.org/pdb/home/home.do) and were determined by the X-ray technique. We used all the available APC crystal structures from eight cyanobacteria and one red alga: 1ALL from *Spirulina platensis* (Brejc et al. 1995), 1B33 from *Mastigocladus laminosus* (Reuter et al. 1999), 2V8A from *Thermosynechococcus elongatus* (Murray et al. 2007), 3DBJ from *Th. vulcanus* (McGregor et al. 2008), 4RMP from *Phormidium* sp. A09DM (Sonani et al. 2015), 4PO5 from *Synechocystis* PCC 6803 (Peng et al. 2014), 4F0U from *Synechococcus elongatus* PCC 7942 (Marx and Adir 2013), 2VJT from *Gloeobacter violaceus*, and 1KN1 from *Porphyra yezoensis* (Liu et al. 1999).

The GROMACS-5.0.6 software (Pronk et al. 2013) was used for geometry optimization of all the molecular models

(trimers, hexamers, and their complexes) with the OPLS-AA forcefield (Jorgensen et al. 1996). The standard pyrrole atom types were used for chromophore molecule model construction. The partial charges of the phycobilin atoms were corrected, according to the RESP procedure (Bayly et al. 1993). Quantum chemistry calculations were carried out in the DFT approximation (B3LYP5 functional and 6-311+G* basis set), using FireFly software (Granovsky 2015).

The mutual orientation of APC monomers, trimers, and hexamers in crystal lattices was reconstructed on the basis of crystallographic symmetry using the standard PyMOL (Schrödinger 2010) *symexp* routine. Spatial alignment of APC structures from different organisms was performed through minimization of the backbone RMSD using the standard algorithm. The absence of deletions in the primary sequence alignment of APCs significantly facilitates this task. The distances between chromophores were unified with the distances between theirs centers of mass using a simple python script and the standard PyMOL routine. The structure of αAPC (UniProt ID: Q01951) from *Synechocystis* PCC 6803 is not resolved. Therefore, it was build up by homology in MODELLER 9.15 software (Webb and Sali 2014) using the structure of α-chains from the crystals 1ALL, 1B33, 1KN1, 2V8A, 3DBJ, 4F0U, 4RMP, and 2VJT as templates. The similarity of the template sequences was 59.0 %, and the average similarity between the templates and the target sequence was 78.3 ± 2.2 %. The MODELLER DOPE estimation for the resulting models lies below the −0.3 level and the backbone RMSD between the resulting model and the template structures was 0.21 ± 0.15 Å. This indicates very high reliability of the resulting αAPC structure. The structure of *β*APC (Q1952) and ApcD (P72870) subunits from *Synechocystis* PCC 6803 in the form of $(ApcD/ApcB)_3$-trimers was resolved with the X-ray technique (Peng et al. 2014). The 3D structure of the PBL_{CM} was resolved in the recent study (Tang et al. 2015). The presented structure contains the homodimer of PBL_{CM} with deleted PB loop. The overall fold of the PBL_{CM} domain in the resulting structure (Tang et al. 2015) and the chromophore conformation are in good agreement with the developed earlier homology-based model of PBL_{CM} from *S. platensis* (Zlenko et al. 2015). Here we used the 3D structures of PBL_{CM} and ApcF from *S. platensis* (Zlenko et al. 2015) as templates for the development of *Synechocystis* PCC 6803 PBL_{CM} (Q55544, 19–232) and ApcF (P74551) 3D structures, correspondingly. Similarity between *S. platensis* and *Synechocystis* PCC 6803 PB domain sequences was 60.6 %, and the MODELLER DOPE estimation for the folded part of the sequences is quite good (below −0.3), while for the unfolded PB loop region is poor (DOPE ∼−0.2). Nevertheless, the average backbone RMSD among the models was 0.10 ± 0.02 Å. The similarity of the *Synechocystis* PCC 6803 and *S. platensis* ApcF sequences was 66.3 %, the DOPE for ApcF model lay in the range between −0.3 and −0.7, and the backbone RMSD was 0.08 ± 0.01 Å.

We used the X-ray structure of PSII from *Th. elongatus* (2AXT, Loll et al. 2005) and of PSI from *S. elongatus* (1JB0, Jordan et al. 2001) for the development of the PBS core supercomplexes with PSII and PSI, respectively. Two different models of PBS core with the photosystems were built using a simple python script that minimized the distances between the centers of mass of PBL_{CM} and ApcD phycobilin chromophores and the nearest chlorophyll molecules.

Results and discussion

There are nine different resolved crystal structures of cyanobacterial APCs, with two of them containing the minor components of PBS core. According to the X-ray diffraction studies, each APC trimer is a convexo-concave disk with approximate diameter of ∼11 nm, thickness of ∼3 nm, and central channel of ∼3.5 nm (Adir 2005). In the crystal lattices APC trimers contact by their convex or concave surfaces forming face-to-face or back-to-back hexamers, respectively (Brejc et al. 1995; Liu et al. 1999). Our examination showed that mutual orientations of APC trimers in nine crystals under consideration correspond to seven different structural types. We took all of them into account, but only the APC crystals with structural similarity to the supramolecular PBS core organization were selected for further examination. Suitable spatial packing of APC trimers in crystal lattices has to contain two motifs that correspond to the required packing of APC trimers in cylinders of PBS core. The first is the stacks of trimers that can be used for cylinder lengthening. The second motif is a flat layer of honeycomb-packed trimers in the lattice. This motif can be used as a model for the lateral packing of the PBS core basal cylinders.

APC crystal structures

Two crystal structures of enumerated above include the minor polypeptides (ApcC and ApcD) although they do not contain trimer flat layers or stacks. 1) The crystal cell of the APC from *M. laminosus* (1B33) contains two trimers and $L_C^{7.8}$ linker polypeptide. The $L_C^{7.8}$ polypeptide appears to be localized inside the trimer cavity. This type of APC trimers has been used directly for reconstruction of the edge trimers of PBS core cylinders. 2) The crystal lattice of APC from *Synechocystis* PCC 6803 (4PO5) with the minor ApcD component contains the ApcD/*β*APC trimers

arranged in flat layers, but the geometry of observed intertrimer contacts does not reflect the PBS core structure.

The coupled parallel layers of trimers are recognized in the crystal lattice of APCs from *Th. elongatus* (2V8A) and *Phormidium* sp. A09DM (4RMP). The spatial structures of these proteins are identical (intertrimer backbone RMSD of 0.39 Å). Besides, the backbone RMSD between the disk triples varies 0.81 Å from 2V8A to 4RMP, which reflects high similarity between the crystal lattices. The trimers in the adjusting layers are faced to each other with their concave surfaces, but the layers themselves are rotated at the angle of 60°, and therefore the trimers do not form hexamers. Two types of disk lateral packing in triples can be recognized in these layers (Fig. 1a, green layer). The first type ("open") is characterized by a large hole between each three adjoining trimers, and the second is characterized by a small hole between them ("closed"). Each type of revealed trimer lateral packing can be considered as a possible model of the three adjusting cylinders packing in the PBS core.

APC crystals from *S. platensis* (1ALL) and *Th. vulcanus* (3DBJ) have the same two types of disk lateral packing as observed in 2V8A and 4RMP, and the trimer spatial structures are similar (RMSD is 0.65 Å). In contrast to the 2V8A and 4RMP, the trimers in 1ALL and 3DBJ are faced to each other with their convex surfaces, and the coupled layers are oriented identically (Fig. 1a). This results in formation of back-to-back hexamers (Fig. 2a), which are identical in both crystals (RMSD of 0.78 Å). Moreover, the trimer lateral packing in both layers of 1ALL and 3DBJ lattices is the same, resulting in two types of hexamer packing: "open" and "closed" (Fig. 1a, green and gray layers). Both types of packing from 1ALL and 3DBJ can be preliminary considered as a model of cylinder packing in the PBS core.

The lattices of the three other APC crystals, 4F0U, 1KN1, and 2VJT, contain face-to-face hexamers whose structures are similar but not identical (RMSD of 1.38 ± 0.08 Å). In the lattice of the APC crystal from *S. elongatus* (4F0U), hexamers do not form lateral or face contacts required for PBS core reconstruction. The lattice of the APC crystal from *P. yezoensis* (1KN1) contains face-to-face hexamers (Fig. 2b) arranged in flat honeycomb layers (Fig. 1b). The hexamer layers can be clearly represented as very close layers of coupled trimers. In each triplet of 1KN1 hexamers, the upper triple of trimers always has "open" lateral packing and the underlying one has "closed" packing, or vice versa (Fig. 1b). In contrast, in 1ALL and 3DBJ structures both triples of trimers in a triplet of hexamers have the same lateral packing. So, there is only one type of hexamer lateral packing in the 1KN1 lattice (Fig. 1b), which can also be considered as a model of lateral arrangement of cylinders in the PBS core.

Crystal lattices of APC from *G. violaceus* (2VJT) contain infinite stacks of trimers, which can be interpreted as trains of face-to-face or back-to-back hexamers. Stacks are regularly sheared in the long axis direction, which leads to disruption of flat lateral packing of trimers. The structure of face-to-face hexamers from 2VJT is similar to the 1KN1 structure (RMSD of 1.27 Å, Fig. 2b, d), while back-to-back hexamers differ from 1ALL and 3DBJ structures (RMSD of 2.88 ± 0.13 Å) by the larger cleft between the adjacent trimers (Fig. 2a, c). The cleft increase is caused by wedging of face-to-face hexamers between back-to-back ones in neighboring stacks and, therefore, cannot reflect the structure of the real PBS core. Moreover, the least

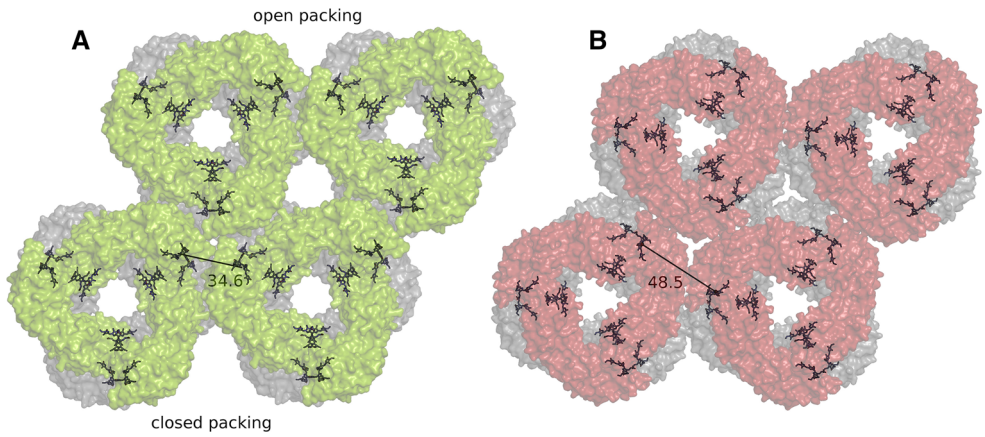

Fig. 1 Lateral packing of APC trimers in crystal lattices. **a** The trimer packing in 2V8A and 4RMP lattices (*green layer*) and the back-to-back hexamer packing in lattices of 1ALL and 3DBJ (*green upper* and *gray lower* layers). **b** The hexamer packing in the 1KN1 lattice. The trimers in *upper* and *lower layers* are rotated and shifted. The *upper layer* of trimers is shown in *color* for clarity. The chromophores are shown with *dark sticks* here and in all figures. The minimal distances between chromophores in adjacent trimers of a layer are 34.6 Å (**a**) and 48.5 Å (**b**)

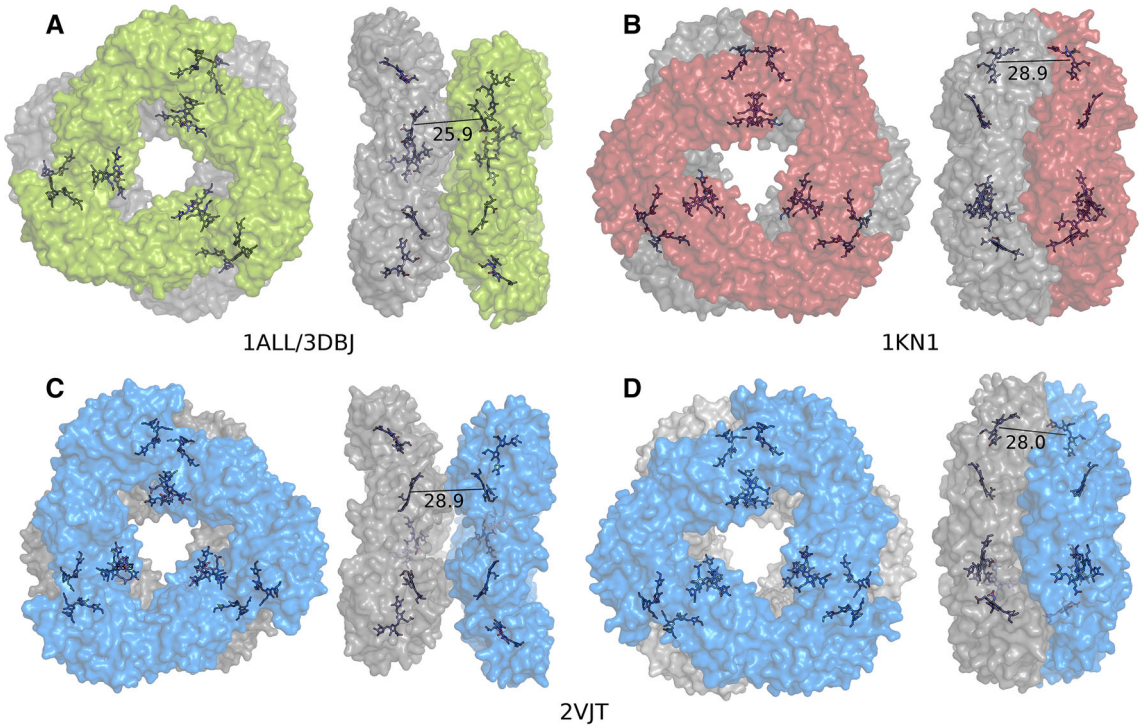

Fig. 2 *Top* and *side* views of APC hexamers. **a** Back-to-back APC hexamers from *S. platensis* (1ALL) and *Th. vulcanus* (3DBJ). **b** Face-to-face hexamers from *P. yezoensis* (1KN1). **c**, **d** Both types of hexamers from *G. violaceus* (2VJT). One trimer in each hexamer is shown in *color* for clarity. The minimal distances (Å) between chromophores in coupled trimers are marked for each structure

measured distance between the chromophores in back-to-back hexamers of 2VJT (28.9 Å) is larger than in 1ALL and 3DBJ lattices (25.9 Å, Fig. 2b, d). Consequently, the rate of energy transfer along the cylinders would be greater in the 1ALL/3DBJ variant of packing. Thus, we have used the back-to-back hexamers from *S. platensis*/*Th. vulcanus* instead of *G. violaceus* for further development of the PBS core model.

PBS core assembling

There are two key points in summarizing our analysis of APC crystal structures. The first is that face-to-back hexamers are absent in all available APC crystals. Such type of intertrimer contact is also unknown for other PBPs (Sidler 1994; Adir 2005). Therefore, face-to-back contacts between APC trimers in the PBS cylinders are hardly possible. The second is that only three ways of lateral packing of hexamers have been identified in the resolved APC crystal structures. Two derive from the trimer packing observed in four structures (1ALL, 3DBJ, 2V8A, and 4RMP; Fig. 1a). The third derives from another type of crystal lattice and was observed only once (1KN1, Fig. 1b). As one of the patterns occurs four times more often than the other, most probably it can occur in PBS core formation. But this argument alone is insufficient for the reconstruction of the PBS core.

While there is no face-to-back contact between APC trimers, we can imagine only two alternative PBS core cylinder compositions: stacked together two back-to-back (Fig. 2a, c) or face-to-face (Fig. 2b, d) hexamers. To choose between these possibilities, we have to analyze the structure of other PBPs and localization of the linker subunits in the PBS core and peripheral rods. The phycocyanin and phycoerythrin in peripheral rods self-assemble only in face-to-face hexamers (Sidler 1994). This suggests that the APCs in PBS core form face-to-face hexamers too. Besides, all linker polypeptides that participate in PBS assembly are localized inside the central cavity of the disks (Watanabe and Ikeuchi 2013). Through the X-ray technique, this was demonstrated for a part of the R-PE γ-subunit (Contreras-Martel et al. 2001) and for the $L_C^{7.8}$ core subunit (Reuter et al. 1999). Localization of linker polypeptides inside the face-to-face hexamers is crucial for the assembly of the entire PBS (Adir 2005). So, the core cylinder composed of two face-to-face hexamers is most probable. Moreover, a recent study confirms this conclusion by docking of the APC trimers into the electron density maps, obtained for an entire PBS by single-particle electron microscopy (Chang et al. 2015).

According to Fig. 1, core cylinders can be brought in line in three different ways. In the first two patterns (from 1ALL/3DBJ, Fig. 1a), the minimal distance between the chromophores in one layer of adjacent trimers is 34.6 Å, while in the third pattern (from 1KN1, Fig. 1b) this distance is larger and equals to 48.5 Å. Thus, it is more than likely that the lateral packing of trimers in *P. yezoensis* APC crystal does not reproduce the natural packing.

The stacking of four APC trimers into a single whole cylinder and lateral packing of three cylinders in the PBS core are highly interrelated. The trimers must be tightly packed and must not intersect on their interfaces. Therefore, the pair of trimers must be stacked face-to-face as in 1KN1 (Fig. 2b); the pair of hexamers in each cylinder must be stacked back-to-back as in 1ALL (Fig. 2a). Besides, the lateral packing of three cylinders must be as in 1ALL (Fig.1a). To meet these conditions, we complemented each trimer from the 1ALL layer of back-to-back hexamers with one trimer from the 1KN1 face-to-face hexamer. As a result, we got a PBS core cylinder resembling the structure of *G. violaceus* APC crystal (Fig. 3a), but it has a narrowed cleft (Fig. 3b).

The three cylinders form a PBS core. Trimers in the APC hexamers are slightly twisted. The angle of the twist in the 1KN1 face-to-face hexamer (+2°) is up to sign equal to the twist angle in the 1ALL back-to-back hexamers (−2°). As the angle modules are equal, rotational orientation of the first and third trimers in a core cylinder are exactly the same. So, all trimers in all layers in the PBS core have the same lateral packing (as in 1ALL/3DBJ, Fig. 1a). Moreover, all back-to-back hexamer contacts are the same (as in 1ALL/3DBJ, Fig. 2a), and all face-to-face contacts of the trimers are also the same (as in 1KN1, Fig. 2b). Therefore, there are no steric clashes in the obtained tightly packed model of PBS core. Since there are two alternative lateral packings of the back-to-back hexamers presented in the 1ALL/3DBJ crystal lattices ("open" and "closed"), we got two alternative PBS core structures (see PBS core structures in Fig. 4).

The PB domain of L_{CM} is located in the second trimer of one of the PBS core basal cylinders and the ApcD subunit is located in the adjacent edge trimer, with account for antiparallel composition of basal cylinders (third and fourth trimers) (Lundell and Glazer 1983; Anderson and Eiserling 1986; Reuter et al. 1990). As the chromophores of PBL_{CM} and ApcD donate the absorbed light energy to chlorophyll, the distance between them and the thylakoid membrane must be as short as possible. So, the PB domain of L_{CM} protein should be located in the second trimer instead of the α-subunit nearest to the membrane plane. The ApcD subunit occupies a similar position in the adjacent edge trimer of each basal cylinder. The β^{18} subunit is known to form a dimer with the PB domain, thus localizing its position in the developed PBS core model (Fig. 4).

"Closed" and "open" models of the PBS core cannot be properly selected on the basis of the crystallographic data. To choose one of the two possibilities, we had to use the electron microscopy data. The PBS core shape examined with single-particle electron microscopy at 13 Å (Arteni et al. 2009) and 20 Å (Chang et al. 2015) resolutions corresponds to the "closed" lateral trimer packing (Fig. 4a).

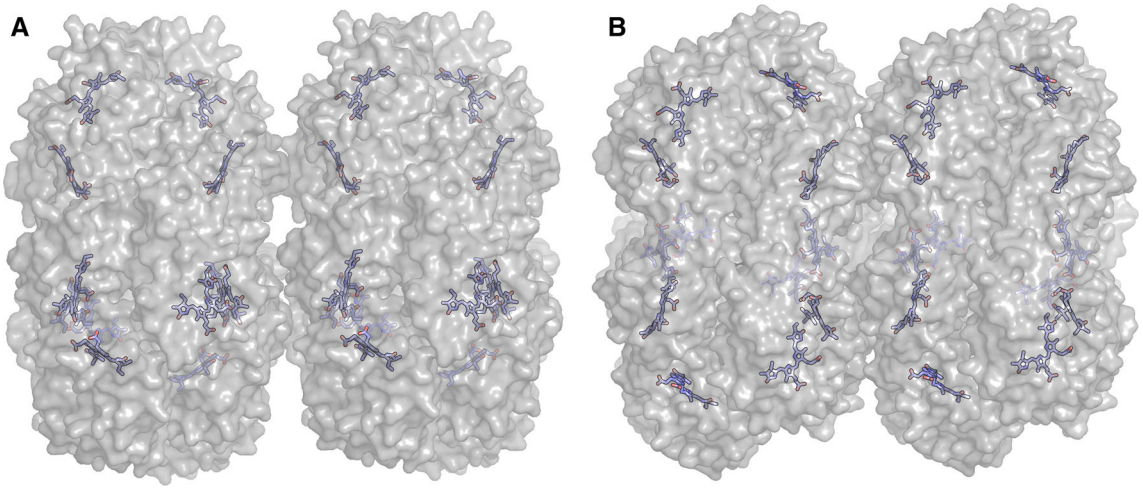

Fig. 3 Models of the PBS core cylinder. **a** Cylinder-like structure revealed in 2VJT crystal lattice. **b** Cylinder structure developed on the basis of 1ALL back-to-back hexamer packing and 1KN1 face-to-face trimer packing. It is clearly seen that the cleft between hexamers in the model (**b**) is remarkably narrower than in the case of the 2VJT crystal lattice (**a**). The enhancement of the interhexamer cleft in 2VJT is the result of tight packing of the APC in the crystal

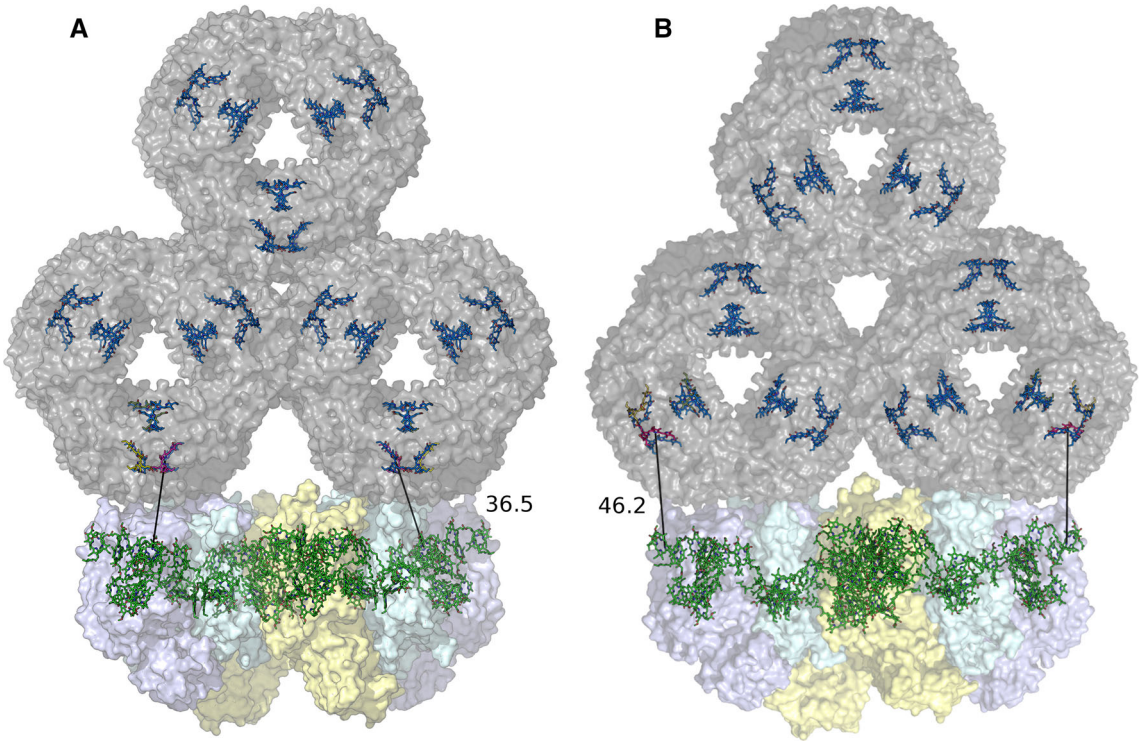

Fig. 4 Face views of "closed" (**a**) and "open" (**b**) PBS core/PSII dimer supercomplex. Surfaces represent: *gray* the PBS core, *violet* CP43 proteins, *cyan* RC proteins, and *yellow* CP47 proteins. Sticks represent: *sky blue* bulk phycobilin chromophores, *pink* PBL_{CM} chromophores, *yellow* ApcD-subunit chromophores, *pea green* β^{18} subunit phycobilins, and *bright green* chlorophylls. The minimal distances between the PBL_{CM} phycobilin and the nearest chlorophyll of CP43 are 36.5 Å in the "closed" and 46.2 Å in the "open" model

Interaction of the PBS core with PSII

PBSs were reasonably assumed to be the external antenna of PSII (Melis 1991; Mimuro et al. 1999). This was demonstrated long ago by the action spectra of photoreaction II (Haxo and Blinks 1950), by 77 K fluorescence excitation spectra of PSII antenna chlorophyll (Ghosh and Govindjee 1966; Fork and Mohanty 1986), and by results of time-resolved fluorescence spectroscopy (Bruce et al. 1985; Yamazaki et al. 1984; Mimuro et al. 1999). The well-known chlorophyll bands at 685 and 695 nm attributed to PSII (Rijgersberg and Amesz 1980; Pakrasi and Sherman 1984; Barber et al. 2003) are known to prevail in low temperature fluorescence emission spectra of cyanobacteria measured under excitation in the PBS absorption region. Preparations consisting of PBSs and fragments of thylakoid membranes capable of oxygen evolution were obtained in vitro by mild detergent treatment along with the spectral data (Gantt et al. 2003; Pakrasi and Sherman 1984). In vivo, PSII exists in the form of dimers (Mörschel and Schatz 1987; Boekema et al. 1995). The area of the proposed PBS core contact with the thylakoid membrane is similar to that of the PSII dimer (Bald et al. 1996).

Normally, the contact between the cyanobacterial PBS core and PSII dimer is depicted as a combination of PBS and PSII face views (Bald et al. 1996; Watanabe and Ikeuchi 2013; Chang et al. 2015). In this study, we have developed the three-dimensional model of the PBS core and the PSII pigment–protein complex from *Synechocystis* PCC 6803, minimizing the distance between phycobilin of the PBL_{CM} and the nearest chlorophyll antenna molecules of PSII. Our data confirm the model of the PBS settling on PSII dimer surface. The directional energy transfer from PBL_{CM} to adjacent chlorophyll molecules strongly depends on the strict order of chromophores in PBS core cylinders and on inter-pigment distances. We tested both "open" and "closed" models of the PBS core. A strong argument in favor of the "closed" packing pattern is the shortest ($\sim$36 Å, Fig. 4a) minimal distance between the nearest phycobilins of the PBS and CP43 antenna chlorophylls of PSII, while the distance between chlorophylls of CP43 and phycobilins of terminal emitters in case of the "open" PBS core model was about 46 Å (Fig. 4b). A similar result of 46 Å was obtained by Chang et al. (2015) for the minimal distance between chromophores in the analogous model. Both distances are compatible for the Forster type of energy transfer, but in the case of the "open" core

structure, the distance is almost at the limit of energy migration possibility. The energy transfer rate in the case of the "closed" model is four times faster than in case of the "open" model. This is an important factor in favor of the "closed" model.

Interaction of the PBS core with PSI

Cyanobacteria and red algae are characterized by relatively high PSI/PSII ratio (Biggins and Bruce 1989). In addition, the core complex of PSI (Jordan et al. 2001) incorporates 2.7 times more chlorophylls than the PSII core Ferreira et al. (2004). The PBS was generally assumed to be employed mainly as an external antenna compensating for both low levels of PSII and the chromophores shortage in it (Melis 1991). However, it was eventually found that part of the energy absorbed by PBS is transferred to PSI. The 77 K chlorophyll emission spectra measured under PBS excitation demonstrate distinct bands at 715–730 nm attributed to PSI, along with common fluorescence peaks of PSII, and the PSI fluorescence excitation spectra exhibit peaks attributed to PBPs (Ghosh and Govindjee 1966; Rijgersberg and Amesz 1980; Zilinskas and Greenwald 1986). Time-resolved 77 K fluorescence spectra of cyanobacteria measured under excitation of PBS show an increase of PSI and PSII chlorophyll emissions along with a decrease of their own fluorescence (Bruce et al. 1985; Yamazaki et al. 1984). Energy transfer from PBS to PSI in cyanobacteria and red algae is revealed by P700 oxidation in the light absorbed by PBS, which was demonstrated by photobleaching at 705 nm and by the EPR signal (Glazer et al. 1994; Mullineaux 1994; Stadnichuk et al. 2011). PBS bands are clearly visible in action spectra of PSI-dependent reversible respiration photoinhibition in various mutants and wild types of cyanobacteria (Wang et al. 1977; Boichenko et al. 1993; Rakhimberdieva et al. 2001). In summary, participation of PBSs in feeding energy to PSI is considered to be proved; however, the possible structure of PBS and PSI complex is a long-standing problem (Liu et al. 2013).

In cyanobacteria, PSI mainly forms trimers with a smaller share of monomers (Chitnis and Chitnis 1993; Kruip et al. 1997). Trimerization of PSI may be disturbed by various environmental conditions (Karapetyan et al. 1999). In contrast to the flat cytoplasmic surface of the PSII dimers (Bald et al. 1996), the surface of the PSI monomers shows a major protrusion of three hydrophilic polypeptide subunits (PsaC, PsaD, and PsaE), which extends into the cytoplasm (Schubert et al. 1997). It was proposed that this protrusion, which does not cover the whole surface of PSI, would prevent tight binding of PBS to PSI (Bald et al. 1996). Binding of PBS to PSI should be mediated by temporal detachment of PBS from PSII (Aspinwall et al. 2004). On the other hand, Liu et al. (2013) reported the isolation of a PBS-PSII-PSI macrocomplexes and suggested that PBS does not need to dissociate from PSII to bind to PSI. Being associated with PSII dimers, PBS was proposed to adjoin the nearest PSI complex with its lateral rodes transferring a part of the absorbed energy (Bald et al. 1996). From our computer modeling, we provide evidence of the existence of a PBS fraction directly attached to PSI monomers in *Synechocystis* PCC 6803. The protein protrusion on the cytoplasmic surface of PSI core complex does not hinder association with the PBS as its size of about 3 nm (Schubert et al. 1997; Neilson and Durnford 2010) ideally fits the cleft between the two bottom cylinders of the PBS core (Fig. 5). Minimal inter-chromophore distance between the phycobilins of PBL_{CM} and ApcD and antenna chlorophylls was determined to be about 30 Å. This is very close to the distance obtained in the PBS-PSII supercomplex (Fig. 4a) and allows effective energy transfer. The same protrusion prevents contact of PSI trimers with the PBS because the threefold symmetry of out of

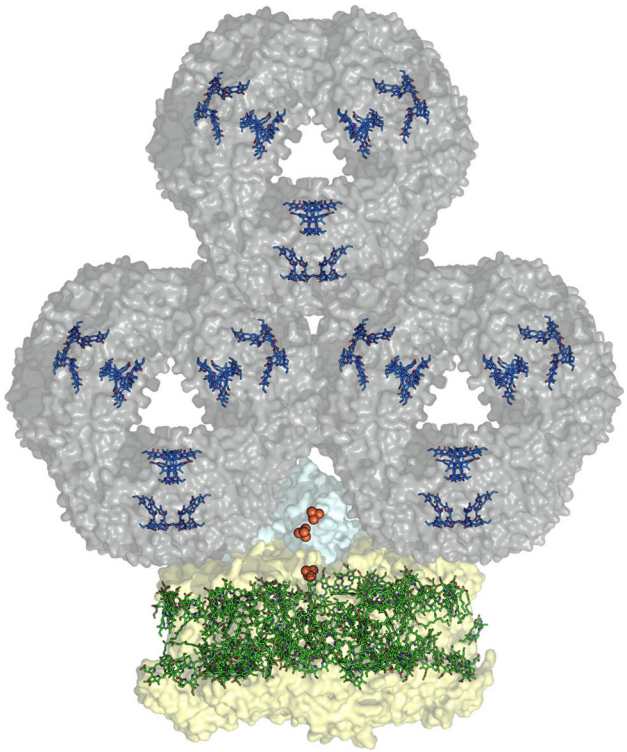

Fig. 5 Proposed complex of PSI monomer and PBS core of the "closed" type. Surfaces represent: *gray* the PBS core, *cyan* the protrusion on the surface of PSI (PsaC, PsaD, and PsaE subunits), and *yellow* the rest of the PSI. *Green sticks* represent the chlorophyll molecules. The *orange spheres* reflect the position of iron atoms in the FeS clusters. It is clearly seen that the shape and size of the protrusion on the PSI surface fits very well in the groove between the basal cylinders of the PBS core of "closed" type. The minimal distance between the chromophores of PBS and PSI is about 30 Å

membrane protrusions in this case cannot match the two-fold symmetry of the PBS core. If this is really so, the PSI trimer/monomer ratio can impact the share of PBS interacting with PSI. Recently, it was demonstrated that specific rod-shaped PBSs including C-phycocyanin, rather than APC, directly form supercomplexes with PSI of *Anabaena* sp. (Watanabe et al. 2014). PSI of the red algae exists in photosynthetic membrane in monomeric form, and interaction with PBSs was shown there by different spectroscopic techniques (Stadnichuk et al. 2011). So, our results confirm the model of the direct interaction of "conventional" PBS (Watanabe and Ikeuchi 2013) with the monomeric PSI in cyanobacteria.

Acknowledgments The work was supported by the Russian Science Foundation, Project Number 14-14-00589.

References

Adir N (2005) Elucidation of the molecular structures of components of the phycobilisome: reconstructing a giant. Photosynth Res 85:15–32

Anderson L, Eiserling F (1986) Asymmetrical core structure in phycobilisomes of the cyanobacterium *Synechocystis* 6701. J Mol Biol 191:441–451

Arteni A, Ajlani G, Boekema E (2009) Structural organization of phycobilisomes from *Synechocystis* strain PCC 6803 and their interaction with the membrane. Biochim Biophys Acta 1787:131–141

Aspinwall C, Sarcina M, Mullineaux C (2004) Phycobilisome mobility in the cyanobacterium *Synechococcus* sp. PCC7942 is influenced by the trimerisation of photosystem I. Photosynth Res 79:179–187

Bald D, Kruip J, Rögner M (1996) Supramolecular architecture of cyanobacterial thylakoid membranes: how is the phycobilisome connected with the photosystems? Photosynth Res 49:103–118

Barber J, Morris E, Foncesca PD (2003) Interaction of the allophycocyanin core complex with photosystem II. Photochem Photobiol Sci 2:536–541

Bayly C, Cieplak P, Cornell W, Kollman P (1993) A well-behaved electrostatic potential based method using charge restraints for deriving atomic charges: the RESP model. J Phys Chem 97:10269–10280

Biggins J, Bruce D (1989) Regulation of excitation energy transfer in organisms containing phycobilins. Photosynth Res 20:1–34

Boekema E, Hankamer B, Bald D, Kruip J, Boonstra A, Barber J, Rögner M (1995) Supramolecular structure of the photosystem II complex from green plants and cyanobacteria. Proc Natl Acad Sci USA 92:175–179

Boichenko V, Klimov V, Mayers S, Barber J (1993) Characterization of the light-induced oxygen gas exchange from the IC 2 deletion mutant of *Synechocystis* PCC 6803 lacking the photosystem II 33 kda extrinsic protein. Z Naturforsch 48C:224–233

Brejc K, Ficner R, Huber R, Steinbacher S (1995) Isolation, crystallization, crystal structure analysis and refinement of allophycocyanin from the cyanobacterium *Spirulina platensis* at 2.3 Å resolution. J Mol Biol 249:424–440

Bruce D, Biggins J, Thewalt M (1985) Mechanism of the light state transition in photosynthesis. IV: Picosecond fluorescence spectroscopy of *Anacystis nidulans* and *Porphyridium cruentum* in state 1 and state 2 at 77 K. Biochim Biophys Acta 806:237–246

Bryant D, Guglielmi G, Tandeau de Marsac N, Castets A, Cohen-Bazire G (1979) The structure of cyanobacterial phycobilisomes: a model. Arch Microbiol 123:113–127

Bryant D (1991) In: Bogorad L, Vasil K (eds) The photosynthetic apparatus: molecular biology and operation. Academic Press, Boston, pp 257–300

Chang L, Liu X, Li Y, Liu C, Yang F, Zhao J, Sui S (2015) Structural organization of an intact phycobilisome and its association with photosystem II. Cell Res 25:726–737

Chitnis V, Chitnis P (1993) Psal subunit is required for the formation of photosystem I trimers in the cyanobacterium *Synechocystis* sp. PCC 6803. FEBS Lett 336:330–334

Contreras-Martel C, Martinez-Oyanedel J, Bunster M, Legrand P, Piras C, Verned X, Fontecilla-Camps J (2001) Crystallization and 2.2 Å resolution structure of R-phycoerythrin from *Gracilaria chilensis*: a case of perfect hemihedral twinning. Acta Crystallogr D Biol Crystallogr 57:52–60

David L, Marx A, Adir N (2011) High-resolution crystal structures of trimeric and rod phycocyanin. J Mol Biol 405:201–213

David L, Prado M, Arteni A, Elmlund D, Blankenship R, Adir N (2014) Structural studies show energy transfer within stabilized phycobilisomes independent of the mode of rod-core assembly. Biochim Biophys Acta 1837:385–395

Ferreira K, Iverson T, Maghlaoui K, Barber J, Iwata S (2004) Architecture of the photosynthetic oxygen-evolving center. Science 303:1831–1838

Fork D, Mohanty P (1986) In: Amesz G, Fork D (eds) Light emission by plants and bacteria. Academic Press, Orlando, pp 451–496

Gantt E, Conti S (1966) Granules associated with the chloroplast lamellae of *Porphyridium cruentum*. J Cell Biol 29:423–434

Gantt E, Grabowski B, Cunningham F (2003) In: Green B, Parson V (eds) Light-harvesting antennas in photosynthesis. Kluwer, New York, pp 307–322

Ghosh A, Govindjee (1966) Transfer of the excitation energy in *Anacystis nidulans* grown to obtain different pigment ratios. Biophys J 82:161–166

Glazer A (1984) Phycobilisome: a macromolecular complex optimized for light energy transfer. Biochim Biophys Acta 768:29–51

Glazer A, Gindt Y, Chan C, Sauer K (1994) Selective disruption of energy flow from phycobilisomes to photosystem I. Photosynth Res 40:167–173

Granovsky A (2015) Firefly version 8.0.0 http://classic.chem.msu.su/gran/firefly/index.html

Haxo F, Blinks L (1950) Photosynthetic action spectra of marine algae. J Gen Physiol 33:389–422

Jordan P, Fromme P, Witt H, Klukas O, Saenger W, Krauss N (2001) Three-dimensional structure of cyanobacterial photosystem I at 2.5 Å resolution. Nature 411:909–917

Jorgensen W, Maxwell D, Tirado-Rives J (1996) Development and testing of the OPLS all-atom force field on conformational energetics and properties of organic liquids. J Am Chem Soc 118:11225–11236

Karapetyan N, Holzwarth A, Rögner M (1999) The photosystem I trimer of cyanobacteria: molecular organization, excitation dynamics and physiological significance. FEBS Lett 460:395–400

Kruip J, Chitnis P, Lagoutte B, Rögner M, Boekema E (1997) Structural organization of the major subunits in cyanobacterial photosystem I. Localization of subunits PsaC, -D, -E, -F, and -J. J Biol Chem 272:17061–17069

Liu H, Jiang T, Zhang J, Liang D (1999) Crystal structure of allophycocyanin from red algae *Porphyra yezoensis* at 2.2 Å resolution. J Biol Chem 274:16945–16952

Liu L, Chen X, Zhang B, Zhou B (2005) Characterization, structure and function of linker polypeptides in phycobilisomes of

cyanobacteria and red algae. Biochim Biophys Acta 1708:133–142
Liu H, Zhang H, Niedzwiedzki D, Prado M, He G, Gross M, Blankenship R (2013) Phycobilisomes supply excitations to both photosystems in a megacomplex in cyanobacteria. Science 342:1104–1107
Loll B, Kern J, Saenger W, Zouni A, Biesiadka J (2005) Towards complete cofactor arrangement in the 3.0 Å resolution structure of photosystem II. Nature 438:1040–1044
Lundell D, Glazer A (1983) Molecular architecture of a light-harvesting antenna. Core substructure in *Synechococcus* 6301 phycobilisomes: two new allophycocyanin and allophycocyanin B complexes. J Biol Chem 258:902–908
Marx A, Adir N (2013) Allophycocyanin and phycocyanin crystal structures reveal facets of phycobilisome assembly. Biochim Biophys Acta 1827:311–318
McGregor A, Klartag M, David L, Adir N (2008) Allophycocyanin trimer stability and functionality are primarily due to polar enhanced hydrophobicity of the phycocyanobilin binding pocket. J Mol Biol 384:406–421
Melis A (1991) Dynamics of photosynthetic membrane composition and function. Biochim Biophys Acta 1058:87–106
Mimuro M, Kikuchi H, Murakami A (1999) Structure and function of phycobilisomes. In: Singhal G, Renger G, Sopory S, Irrgang K, Govindjee (eds) Concepts in photobiology: photosynthesis and photomorphogenesis. Narosa Publishing House, New Delhi, pp 104–135
Mörschel E, Schatz G (1987) Correlation of photosystem II complexes with exoplasmatic freeze-fracture particles of thylakoids of the cyanobacterium *Synechococcus*. Planta 172:145–154
Mullineaux C (1994) Excitation energy transfer from phycobilisomes to photosystem I in cyanobacterial mutant lacking photosystem II. Biochim Biophys Acta 95:175–182
Murray J, Maghlaoui K, Barber J (2007) The structure of allophycocyanin from *Thermosynechococcus elongatus* at 3.5 Å resolution. Acta Crystallogr Sect F Struct Biol Cryst Commun 63:998–1002
Neilson J, Durnford D (2010) Structural and functional diversification of the light-harvesting complexes in photosynthetic eukaryotes. Photosynth Res 106:57–71
Pakrasi H, Sherman L (1984) A highly active oxygen-evolving photosystem II preparation from the cyanobacterium *Anacystis nidulans*. Plant Physiol 74:724–745
Peng P, Dong L, Sun Y, Zeng X, Ding W, Scheer H, Yang X, Zhao K (2014) The structure of allophycocyanin B from *Synechocystis* PCC 6803 reveals the structural basis for the extreme redshift of the terminal emitter in phycobilisomes. Acta Crystallogr D Biol Crystalogr 70:2558–2569
Pronk S, Pall S, Schulz R, Larsson P, Bjelkmar P, Apostolov R, Shirts M, Smith J, Kasson P, van der Spoel D, Hess B, Lindahl E (2013) GROMACS 4.5: a high-throughput and highly parallel open source molecular simulation toolkit. Bioinf 29:845–854
Rakhimberdieva M, Boichenko V, Karapetyan N, Stadnichuk I (2001) Interaction of phycobilisomes with photosystem II dimers and photosystem I monomers and trimers in the cyanobacterium *Spirulina platensis*. Biochemistry 40:15780–15788
Reuter W, Nickel C, Wehrmeyer W (1990) Isolation of allophycocyanin B from Rhodella violacea results in a model of the core from hemidiscoidal phycobilisomes of rhodophyceae. FEBS Lett 273:155–158
Reuter W, Wiegand G, Huber R, Than M (1999) Structural analysis at 2.2 Å of orthorhombic crystals presents the asymmetry of the allophycocyanin-linker complex, AP · $L_C^{7.8}$ from phycobilisomes of *Mastigocladus laminosus*. Proc Natl Acad Sci USA 96:1363–1368
Rijgersberg C, Amesz J (1980) Fluorescence and energy transfer in phycobiliprotein-containing algae at low temperature. Biochim Biophys Acta 592:261–271
Schrödinger L (2010) The PyMOL molecular graphics system, version 1.3r1
Schubert W, Klukas O, Saenger W, Fromme P, Witt H (1997) Photosystem I of *Synechococcus elongatus* at 4 Å resolution: comprehensive structure analysis. J Mol Biol 272:741–769
Sidler W (1994) In: Bryant D (ed) The molecular biology of cyanobacteria. Kluwer, Dordrecht, pp 139–216
Sonani R, Gupta G, Madamwar D, Kumar V (2015) Crystal structure of allophycocyanin from marine cyanobacterium *Phormidium* sp. A09DM. PLOS ONE 10(e0124):580
Stadnichuk I, Bulychev A, Lukashev E, Sinetova M, Khristin M, Jonson M, Ruban A (2011) Far-red light regulated efficient energy transfer from phycobilisomes to photosystem I in the red microalga Galdieria sulphuraria and photosystem-related heterogeneity of phycobilisome population. Biochim Biophys Acta 1807:227–235
Stadnichuk I, Krasilnikov P, Zlenko D (2015) Cyanobacterial phycobilisomes and phycobiliproteins. Microbiology 84:131–141
Tang K, Ding W, Höppner A, Zhao C, Zhang L, Hontani Y, Kennis J, Gärtner W, Scheer H, Zhou M, Zhao K (2015) The terminal phycobilisome emitter, L_{CM}: a light-harvesting pigment with a phytochrome chromophore. Proc Natl Acad Sci 112:15880–15885
Wang R, Stevens C, Myers J (1977) Action spectra for photoreactions I and II of photosynthesis in the blue-green alga *Anacystis nidulans*. Photochem Photobiol 6:103–108
Watanabe M, Ikeuchi M (2013) Phycobilisome: architecture of a light-harvesting supercomplex. Photosynth Res 116:265–276
Watanabe M, Semchonok D, Webber-Birungi M, Shigeki E, Kondo K, Narikawa R, Ohmori M, Boekema E, Ikeuchi M (2014) Attachment of phycobilisomes in an antenna photosystem I super-complex of cyanobacteria. Proc Natl Acad Sci 111:2512–2517
Webb B, Sali A (2014) Comparative protein structure modeling using MODELLER. Curr Protoc Bioinformatics 5:5.6.1–5.6.32
Yamazaki I, Mimuro M, Murao T, Yamazaki T, Yoshihara K, Fujita Y (1984) Excitation energy transfer in the light harvesting antenna system of the red alga *Porphyridium cruentum* and the blue-green alga *Anacystis nidulans*: analysis of time-resolved fluorescence spectra. Photochem Photobiol 39:233–240
Zilinskas B, Greenwald L (1986) Phycobilisome structure and function. Photosynth Res 10:7–35
Zlenko D, Krasilnikov P, Stadnichuk I (2015) Role of inter-domain cavity in the attachment of the orange carotenoid protein to the phycobilisome core and to the fluorescence recovery protein. J Biomol Struct Dyn. doi:10.1080/07391102.2015.1042913